Flume investigation of the interaction mechanisms between debris flows and slit dams

H. S. Hu [a,b]*, Gordon G. D. Zhou [a,b], D. Song[a,b]

[a] *Key Laboratory of Mountain Hazards and Earth Surface Process/Institute of Mountain Hazards and Environment, Chinese Academy of Sciences (CAS), #.9, Block 4 , Renminnanlu Road, Chengdu, 610041,China*
[b] *University of Chinese Academy of Sciences, No.19(A) Yuquan Road, Shijingshan District, Beijing, 100049, China*

Abstract

Slit dams are designed to mitigate debris-flow hazards. However, according to field surveys and past experimental studies, slit dams constructed using currently prescribed design methods usually become blocked, which then leads to the loss of capacities of the slit dam's capability to mitigate debris-flow hazards. In this study, a series of flume tests were conducted to investigate the interaction mechanisms between debris flows and slit dams. This work aims to contribute to the design of slit dams more reliable. The influence of debris-flow water content (w) and the slit-dam relative post spacing b/d_{max} (b: post spacing; d_{max}: maximum particle diameter) were examined. Experimental results reveal that when w<22%, dead zones and pile-ups occur during the interaction processes. When w≥22% and b/d_{max}≤2.3, run-up, overtopping, and backwater effects can be observed, and with no apparent formation of dead zones. Moreover, when w≥26% and b/d_{max}>2.3, majority of the granular-water mixtures pass through the slit dam in the form of jet flows with no obvious overtopping.

Keywords: Debris flow; slit dam; interaction mechanisms; flume tests;

1. Introduction

Slit dams, as one type of open-type dams, designed with one or several vertical opening(s) (Chanson, 2004), are initially designed to retain large particles and weaken the peak discharge (Lien et al., 2000; Choi et al., 2018). The relative post spacing (b/d_{max}, b: post spacing, d_{max}: maximum particle diameter) is the key parameter (Johnson and McCuen, 1989; Lien et al., 2003), which directly affects the trapping or regulation function of a slit dam. Mizuyama et al. (1988) and MLR (2004) recommended that b/d_{max} should be between 1.5 and 2.0 for design of slit dams.

However, experimental results from Lin et al. (1988) revealed that slit dams have notable effect on trapping debris materials when b/d_{max}≤1.7. Furthermore, Han and Ou (2006) reported that when b/d_{max}<1.5, the slit dams become prone to blockage. In addition, field investigations (Shima et al., 2016) showed that slit dams are more likely to be filled up by granular materials contained in debris flows when the relative post spacing is narrower (b/d_{max}≈1.5). This effectively diminishes the trapping capacity of a slit dam (Fig.1a and Fig.1b). The results from both engineering practice and past experimental studies have shown that slit dams will be blocked with condition of b/d_{max}≤1.5~2.0, and it will trap granular materials contained in debris flows until the trapping capacity is lost. Ideal behavior of slit dams is to weak the peak discharge of debris flow while is not to be blocked rapidly. Accordingly, the interaction mechanisms between debris flows (with different water contents) and slit dams (with different post spacings) are investigated, which contributes to improving the reliability of slit dams designing.

Fig. 1 Slit dam filled up by granular materials (the pictures from Shima et al., taken in Rishiri island, Japan, 2016)

* Corresponding author e-mail address: *huhongsen15@mails.ucas.ac.cn*

2. Flume model tests

2.1. Scaling

Small-scale flume modelling is widely adopted to investigate the complex flow interaction between mass movement and structures (Choi et al., 2014; Ng et al., 2015), since it can provide a controlled and systematic manner to study mechanisms of flow-structure interaction (Choi et al., 2015). The Froude number (*Fr*), which macroscopically quantifies the ratio of the inertial to gravitational forces, is widely adopted to characterize the dynamic similarity between channelized granular flows (Chehata et al., 2003; Hauksson et al., 2007) and geophysical flows (Hübl et al., 2009; Choi et al., 2015). It can be expressed as (Choi et al., 2015):

$$Fr = \frac{v}{\sqrt{gh\cos\theta}} \qquad (1)$$

where v is the frontal velocity, g is the gravitational acceleration, h is the maximum approaching flow depth (because the damage of structures usually appeared when debris flows approach with maximum flow depth), and θ is the inclination of the channel.

2.2. Model setup and instrumentation

The experiments were carried out using a flume model with an overall length of 7.0 m, a channel width of 0.3 m, and depth of 0.35 m. Figure 2a shows the flume, which consists of a storage tank, a channel with two different inclinations, and a deposition section. The upper part of the channel with has a steeper angle and is usually regarded as the transportation zone. The lower part is the deposition zone. A model of the slit dam was installed 2.8 m upstream of the outflow plain (Fig. 2b). The slit dam consists of three posts. The post spacing of the modelled slit dam varies from 27 mm to 72 mm by decreasing thickness of the posts.

To measure the flow depth of the debris flows, three laser sensors (Leuze, ODSL 30/V-30M-S12, named Lasers A to C) with a resolution of 1 mm were used at the monitoring sections A, B, and C. Meanwhile, three cameras (SONY FDR-AX40, named camera A to C) with a resolution of 1440×1080 pixels and a frame rate of 25 frames per second (fps) were fixed to capture the kinematics of the tests. Three grid lines, with intervals of 0.01 m, were drawn at the base of the channel at sections A, B, and C to approximate the frontal velocity of the flow using the high-speed cameras. In addition, a fourth camera (Nikon D 610, named camera D), with a resolution of 1280×720 pixels and a frame rate of 60 fps, was positioned at the side of the flume to capture the interaction process between debris flows and slit dams. One differential strain-gauge pore pressure transducer (PPT, model KPSI 735, 0 ~ 18 kPa) was used to record the variation in the pore water pressure of debris flows.

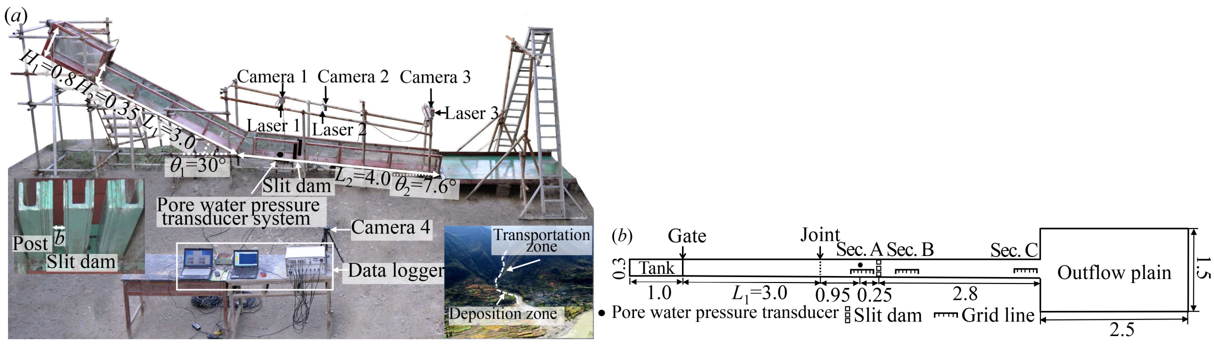

Fig. 2 Setup of flume model tests. (a) side view of flume model; inset on the left: model slit dam; inset on the right: a natural debris flow channel in Kangding county, Sichuan, China; (b) plan view of flume model; (all dimensions in m)

2.3. Experimental materials and program

The granular materials used in the tests were obtained from the debris-flow deposition fan of the Jiangjia Ravine, in the Dongchuan District of Yunnan Province, China. The granular material with diameters larger than 20 mm were removed to make sure that all particles flow smoothly in the flume (Cui et al., 2015). Figure 3 shows the topographic map of Jiangjia Ravine, the sample collecting site, and the grain-size distribution of the granular material used for the tests. The bulk density of the granular materials was measured to be 2680 kg/m³ in the laboratory. Sixty-five kg dry granular material was used in each test.

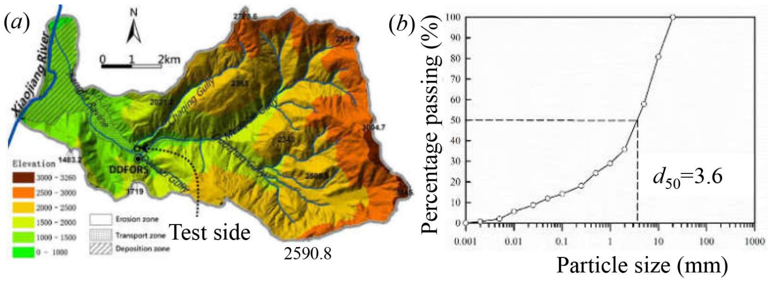

Fig. 3 (a) The topographic map of Jiangjia Ravine in Yunnan province and the sample collecting site; (b) particle size distribution of the granular material

The water content of the debris flows and the relative post spacing were varied to discern their influence on the flow-dam interaction. The range of water contents that were used in the experiments was selected based on trial and error. When the water content of debris flow is less than 18% (15% adopted), the granular-water mixture is not yet considered to be saturated. The velocity of the flow is very low and the debris stops upslope of the slit dam. On the other hand, when the water content of debris flow is greater than 38% (40% adopted), the *Fr* of the approaching flow becomes higher than 8.5, exceeding the common *Fr* range of natural debris flows. Therefore, the water content is varied from 18% to 38% with an interval of 4%. Narrow relative post spacings were set to be $b/d_{max} < 2.0$ (*i.e.*, b/d_{max} = 1.4 and 1.8) while wide relative post spacings varying from 2.3 to 3.6. Details of the modelling tests were summarized in Table 1.

Table 1. Test program of debris flow-slit dam interaction

Test ID	Relative post spacing b/d_{max}	Water content W (%)	Bulk density (kg/m³)	Solid concentration (C_s)	Degree of liquefaction σ_w/σ_t	Approach velocity (m/s)	Flow depth (m)	Froude number Fr
w18-1.4	1.4	18	2160	0.69	0.17	1.56	0.056	2.11
w18-1.8	1.8					1.62	0.056	2.19
w18-2.3	2.3					1.42	0.070	1.72
w18-2.7	2.7					1.39	0.073	1.65
w18-3.1	3.1					1.70	0.061	2.21
w18-3.6	3.6					1.65	0.070	2.00
w22-1.4	1.4	22	2010	0.63	0.45	3.00	0.045	4.53
w22-1.8	1.8					3.25	0.035	5.57
w22-2.3	2.3					3.25	0.035	5.57
w22-2.7	2.7					3.00	0.039	4.87
w22-3.1	3.1					3.00	0.040	4.81
w22-3.6	3.6					3.08	0.043	4.76
w26-1.4	1.4	26	1970	0.59	0.55	3.25	0.043	5.02
w26-1.8	1.8					3.38	0.040	5.42
w26-2.3	2.3					3.50	0.036	5.92
w26-2.7	2.7					3.38	0.036	5.71
w26-3.1	3.1					3.38	0.040	5.42
w26-3.6	3.6					3.33	0.040	5.34
w30-1.4	1.4	30	1920	0.56	0.59	3.50	0.049	5.07
w30-1.8	1.8					3.62	0.050	5.19
w30-2.3	2.3					3.88	0.044	5.93
w30-2.7	2.7					3.75	0.041	5.94
w30-3.1	3.1					3.88	0.040	6.22
w30-3.6	3.6					3.50	0.046	5.23
w34-1.4	1.4	34	1880	0.53	0.65	4.00	0.040	6.41
w34-1.8	1.8					3.88	0.046	5.80
w34-2.3	2.3					4.00	0.043	6.18
w34-2.7	2.7					4.00	0.044	6.11
w34-3.1	3.1					4.12	0.036	6.96
w34-3.6	3.6					4.00	0.046	5.98
w38-1.4	1.4	38	1830	0.50	0.83	4.12	0.049	5.97
w38-1.8	1.8					4.25	0.045	6.42
w38-2.3	2.3					4.12	0.036	6.96
w38-2.7	2.7					4.25	0.039	6.90
w38-3.1	3.1					4.25	0.042	6.65
w38-3.6	3.6					4.00	0.043	6.18

3. Observed interaction process between debris flow and slit dam

In this study, two typical water contents (i.e., *w*=18%, *w*=30%) and two typical relative post spacings (i.e., b/d_{max} =1.4, b/d_{max}=3.1) were chosen to illustrate the interaction processes between debris flows and slit dams, which contributes to the understanding of the interaction mechanisms between slit dams and debris flows.

3.1. Interaction process between slit dam and debris flows with low water content

Debris flows with low water contents (low *Fr* condition), such as those in *w*18-1.4, approach the slit dam with narrow relative post spacing. The debris-flow front is thin and wedge-shaped. It approaches slit dam at *t* =0 s (Fig. 4a) and impacts the slit dam at *t* = 0.22 s. The measured frontal velocity is 1.56 m/s (Fig. 4b). When the front of the debris flow impacts the slit dam, few debris are observed to pass through while the majority of the debris are retained. Sediments depositing behind the slit dam form a dead zone (a region in which the debris are static). At *t* = 0.35 s, the trajectory of the flow started to change as a thin layer of run-up (the debris layer keep running while its height increasing) develops before the slit dam (Figs. 4c&d). As the interaction proceeds, more debris pile up (debris accumulation) on top of the dead zone (Fig. 4e). The pile-up stops when the sediments reach the highest point of the flow (Fig. 4f). Afterwards, the deposited mass begins to propagate upstream along the surface of dead zone (Fig. 4g). The deposits eventually reach a static state at *t* = 1.33 s (Fig. 4h).

Figure 5 shows the interaction between debris flows with a low water content *w*=18% (low *Fr* condition) and a slit dam with wide relative post spacing b/d_{max} = 3.1. The interaction process observed in this test was similar to that observed in test *w*18-1.4 (Fig. 4) as previously discussed, including the tapered approaching debris flow with a measured frontal velocity of 1.70 m/s, impacting on the slit dam (Fig. 5a&b), runs-up (Fig. 5c&d), and piles-up on top of the dead zone (Fig. 5e), backflows (Fig. 5f), and eventually assumes a static state (Fig. 5h). When the debris flow impacts on the slit dam, much more of granular material-water mixture pass through the posts of slit dam. In addition, a weaker backflow was observed in this test as compared to that of *w*18-1.4.

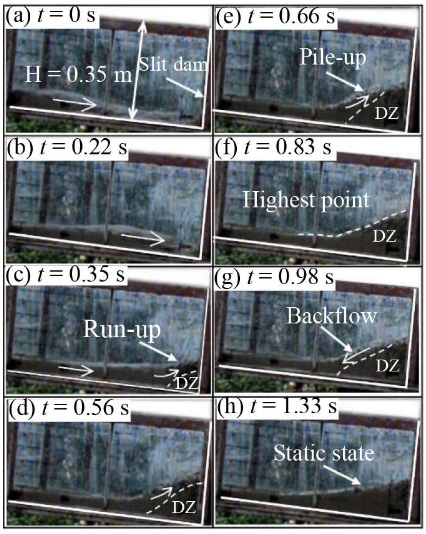

Fig. 4 Interaction process between debris flow with low water content (*w*=18%) and slit dam with narrow relative post spacing (b/d_{max}=1.4): test *w*18-1.4. DZ represents "dead zone".

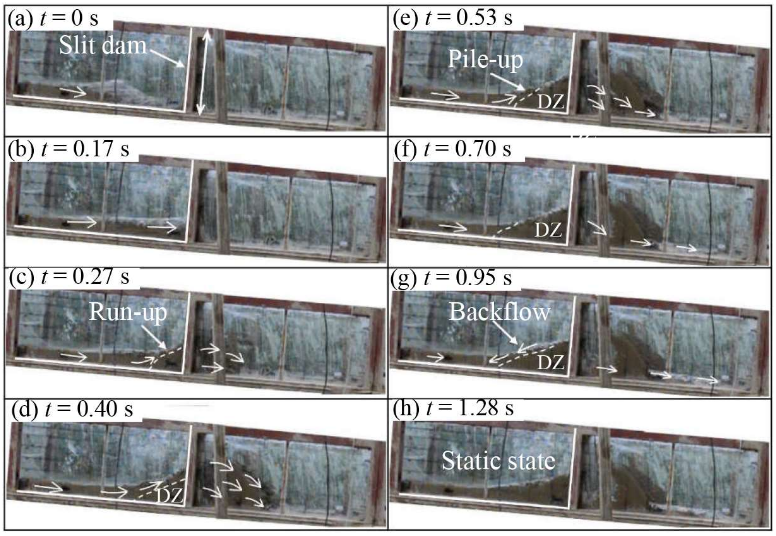

Fig. 5 Interaction process between debris flow with low water content (*w*=18%) and slit dam with wide relative post spacing (b/d_{max}=3.1): test *w*18-3.1. DZ represents "dead zone".

3.2. Interaction process between slit dam and debris flows with high water content

Debris flows with high water contents (high *Fr* condition) were set to impact the slit dams with narrow relative post spacings. Taking the test *w*30-1.4 as an example, a thinner debris-flow front with a larger velocity of 3.5 m/s approaches the slit dam at *t* = 0 s (Fig. 6a). Upon impacting the slit dam, part of the debris flow, the main of the slurry, passes through the slit dam and develops a distinct run-up along the face of the slit dam (Figs. 6b&c). Overtopping is observed at *t* = 0.26 s (Fig. 6c) and *t* = 0.43 s (Fig. 6d). Run-up continues to overtop the slit dam and the run-up region becomes thicker (Fig. 6d). Meanwhile, backward rolling occurs in the run-up region, where part of debris flow hits the posts of the slit dam and is bounced backward (Fig. 6d). The vertical jet begins to fall down towards the channel base (Fig. 6e). At t = 0.93 s, more distinct falling towards the channel base is observed, as well as a bouncing phenomenon which happens when the granular-water mixtures splatter against the channel base (Fig. 6f). Then the granular material-water mixtures upstream of the slit dam start to flow back, increasing the flow's depth (Fig. 6g). Finally, the slit dam retains the sediments, and the slurry contained in the granular material-water mixtures flows through the slit dam (Fig. 6h).

Debris flows with high water contents (high Fr condition) were also set to impact on the slit dam with wide relative post spacings. Taking the test w30-3.1 for example, the measured frontal velocity of a thin debris flow was 3.9 m/s (Fig. 7a). The debris flow makes impact on the slit dam and more of the granular material-water mixture flow through the post spacing. Meanwhile, run-up is observed to develop (Fig. 7b), but was not distinctly thicker than that observed in test w30-1.4 (Figs. 7c&d). No apparent overtopping was observed. At t = 0.67 s, backward rolling occurs (Fig. 7e), which leads to a bouncing phenomenon upstream of the slit dam and is accompanied by the falling of the debris flow down into the channel base downstream of the slit dam (Fig. 7f). Then, the granular material-water mixture upstream of the slit dam start to flow back (Fig. 7g). Finally, majority of the sediment flow through the post spacing, leaving behind a relatively low fraction of its volume behind the slit dam (Fig. 7h).

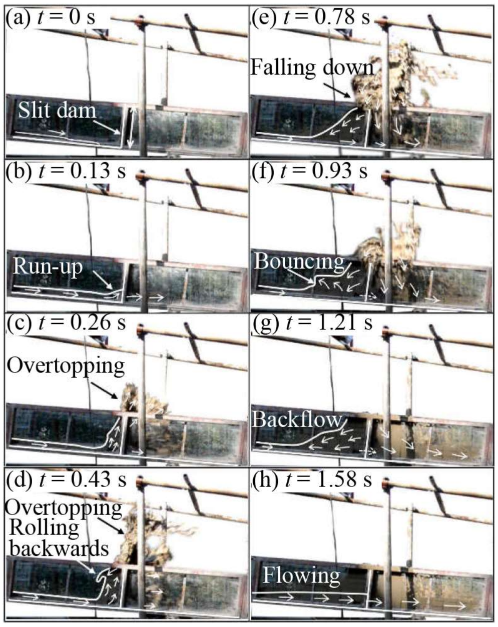

Fig. 6 Interaction process between debris flow with high water content (w=30%) and slit dam with narrow relative post spacing (b/d_{max}=1.4): test w30-1.4.

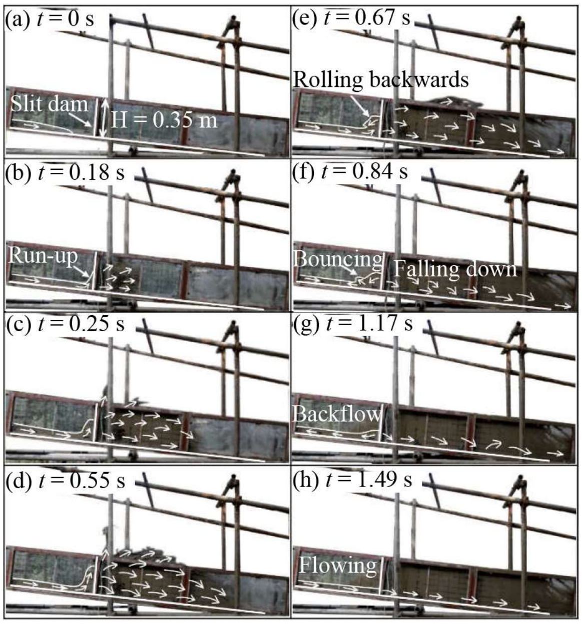

Fig. 7 Interaction process between debris flow with high water content (w=30%) and slit dam with wide relative post spacing (b/d_{max}=3.1): test w30-3.1.

4. Interaction process influenced by water content and relative post spacing

4.1. Influence of water content on interaction process

Comparing Fig. 4 with Fig. 6, with the same b/d_{max}=1.4, the difference in the interaction process is obvious. With a water content of 18%, debris flow-slit dam interaction phenomena such as run-up, dead zone, pipe-up, and backflow are observed. However, when the water content is increased to 30%, additional interaction processes such as overtopping, backwater effect, and bouncing (happens in the form of sediments splash down to the base of the flume) are observed. It is also noted that there is no formation of dead zones. Similarly, set-ups with water contents of 18% (Figs. 5) and 30% (Figs. 7) with relative post spacing of 3.1 are compared. The main interaction processes observed in Fig. 5 are very much similar to those in Fig. 4. The case in Fig. 7 however, shows a much more violent interaction process as debris flows impact the slit dam. Most of its content fly through the slit dam with only a small portion of the debris flow running up along the posts of slit dam and then falling back down to the base of the flume, causing a bouncing phenomenon (Fig. 7f).

Figure 8 show the different interaction processes caused by different water contents that are varied from 18% to 38% and the relative post spacing is 1.8. Here it is observed, that overtopping or run-up are at their highest points. It is noted that when the water content of debris flow is 18% (Fig. 8a), no overtopping phenomenon is observed. However, when $w \geq 26\%$, there is distinct overtopping. Moreover, the height of overtopping increases with the increasing water content.

4.2. Influence of relative post spacing on interaction process

Cases where the debris-flow water contents are both kept at 18%, while the b/d_{max} is increased from 1.4 (Figs. 4) to 3.1 (Figs. 5) are compared to isolate the influence of the relative post spacing. The interaction processes are almost identical, except that more debris passes through the slit dam when b/d_{max} is wider. Similarly, comparing Fig. 6 with Fig. 7, the water contents of debris flow are kept at 30% and the b/d_{max} also increases from 1.4 to 3.1. The differences in these two tests are obvious. In test *w*30-1.4, apparent run-up, overtopping, backwater effect, and bouncing after the debris flow falls down to the base of the flume are observed. In contrast, in test *w*30-3.1, due to the wider b/d_{max}, more debris pass through the slit dam in a jet flow manner, and no overtopping phenomenon is observed. The run-up and bouncing phenomena are still observed but are not as obvious as compared with those in test *w*30-1.4.

The different interaction processes caused by different b/d_{max} are also shown in Fig. 9, where the water contents are kept at 30% and the b/d_{max} is increased from 1.4 to 3.1. In these cases, overtopping or jet flow are at their highest. When $b/d_{max} \leq 2.3$, overtopping after the debris flow makes impact on the slit dam dominates. Increasing b/d_{max}, decreases the height of the run-up (h_e). However, when $b/d_{max} > 2.3$, majority of the granular material-water mixture pass through the slit dam as a jet flow and no obvious overtopping is observed.

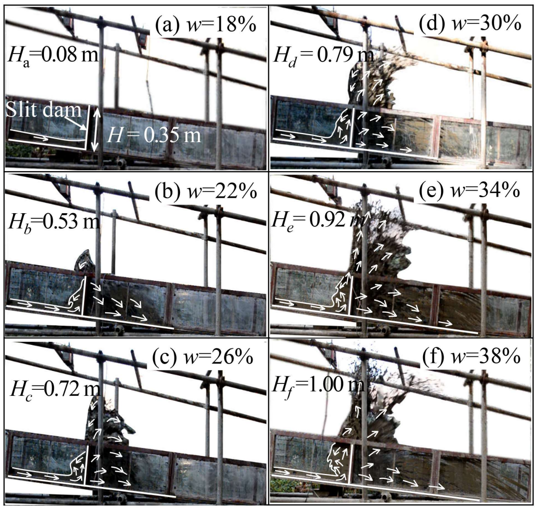

Fig. 8 Snapshots of each test when the overtopping or run-up is at its highest point. Relative post spacing is kept at 1.8 while the water content is varied from 18% to 38% at an interval of 4%.

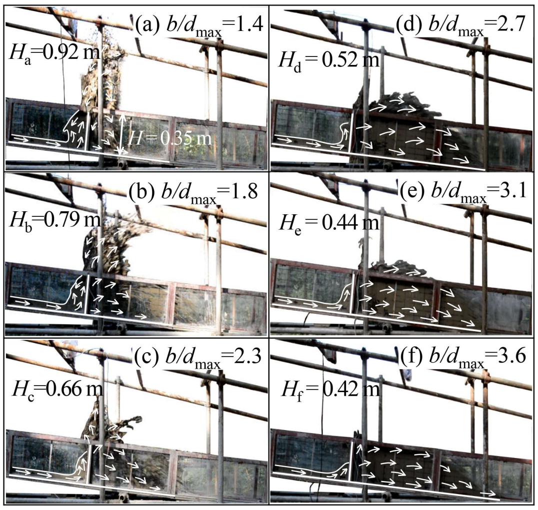

Fig. 9 Influence of the relative post spacing on the interaction process between debris flow and slit dam. Water content is kept at 30% and the relative post spacing ranges from 1.4 to 3.6.

5. Influence of water content and relative post spacing on the height of run-up

Overtopping phenomenon occurs after the interaction between debris flows and slit dams. This potentially causes the foundation of dams to be eroded and result in structural instability (Pan et al., 2013). The degree of overtopping is determined by the height of run-up. Accordingly, it is imperative to ascertain the height of run-up after the interaction between debris flow and slit dam. In this study, the influence of water content and relative post spacing on the height of run-up is investigated. The height of the run-up (h_e) is normalized by the depth of approaching flow (h). This value is named the relative run-up height (h_e/h).

Figure 10 shows the relationship between the relative run-up height (varying water contents) and the relative post spacing. When the relative post spacing is constant, the relative height of run-up increases with the water content. When $w \geq 22\%$, the relative run-up height decreases with the increasing relative post spacing. Indeed, the relative run-up height reaches its maximum value (about 30) when w=38% and $b/d_{\max}$=1.4. For debris flow with w=18%, the relative run-up height is obviously lower than those with w≥22%, and the influence of the relative post spacing on the relative run-up height is negligible. It is also noticed that the overtopping phenomenon is more likely to occur when w≥22% than when w=18%.

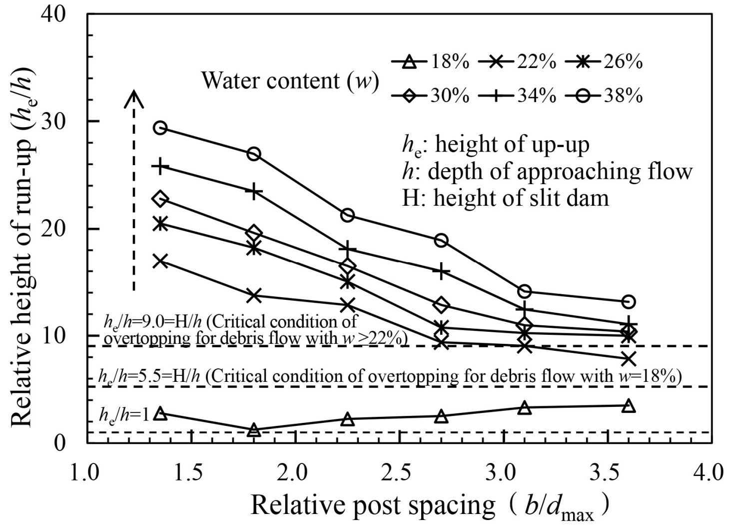

Fig. 10 The relationships between relative run-up height (h_e/h) and relative post spacing ($b/d_{\max}$) for different water contents; h_e: height of run-up.

6. Interaction mechanisms between debris flows and slit dams

Based on the analysis of the interaction processes between debris flows and slit dams, it is evident that water content w and relative post spacing $b/d_{\max}$ are two key variables influencing the interaction mechanisms. Hürlimann et al. (2015) demonstrated, through laboratory experiments, that water content strongly influences the run-out distance of debris flows. In fact, water content essentially reflects the degree of liquefaction of debris flows. The degree of liquefaction, which is defined as the ratio of pore water pressure (σ_w) to the total normal stress of debris flow (σ_t), is used to represent the normalized influence of basal pore pressure on Coulomb resistance (Iverson et al., 2010). The total normal stress (σ_t) was estimated by the bulk density and approaching flow depth, that is $\sigma_t \approx \rho g h cos\theta$, where g is the gravitational acceleration; and θ is the inclination of the channel (Iverson et al., 2010). Both flume experiments (Iverson, 1997; 2010) and field observation (McArdell et al., 2007) suggested that the basal fluid water pressure (proportional to the degree of liquefaction) contributes to the mobility of debris flows.

With lower degree of liquefaction, the grain-contact effective stress dominates. Force chains form much easier and the internal shearing of solid grains is enhanced. From the energy point of view, energy dissipation efficiency of the grain-contact effective stress is much higher than the viscous stress of the liquid phase. Accordingly, debris flows approach the slit dam with a lower velocity. This explains why, when w<26%, the debris flow with a lower velocity impacts on the slit dam, no distinct overtopping is observed, and the trapping capacity of slit dam is obviously influenced by $b/d_{\max}$.

On the contrary, with high degree of liquefaction, the effective stress of debris flows decreases, and debris flows are more fluid-like. Thus the basal resistance becomes minor, leading to higher mobility of debris flows. In addition, solid inertial force dominate during the movement, resulting in highly energetic debris flows. Accordingly, when w≥26%, debris flows with higher velocities impact the slit dam. When $b/d_{\max}$ is narrow, the granular-water mixtures can run up and overtop the slit dam. This further explains why when water content w≥26%, the influence of relative post spacing $b/d_{\max}$ on the trapping capacity is less obvious.

7. Conclusions

A set of flume experiments were carried out to study the interaction mechanisms between slit dams and debris flows. The key findings that can be drawn from this study are:

(1) The relative post spacing and water content govern the interaction mechanisms of slit dams and debris flows. When water content w<22%, pile-up occurs and no distinct overtopping is observed, showing that the

trapping capacity of the slit dam is obviously influenced by b/d_{max}. When $w\geq22\%$ and the relative post spacing $b/d_{max}\leq2.3$, run-up, overtopping, and backwater effects are apparent, and dead zones do not form. The trapping capacity of slit dam is obviously influenced by water content. Moreover, when $w\geq26\%$ and $b/d_{max}>2.3$, majority of the granular material-water mixtures pass through the slit dam in the form of a jet flow and no obvious overtopping phenomenon is observed.

(2) The run-up height reaches its maximum value (about 30) when w=38% and b/d_{max}=1.4. The relative run-up height is obviously lower for debris flows with w=18%, than those with $w\geq22\%$, and the influence of the relative post spacing on the relative height of run-up is negligible.

(3) The degree of liquefaction (σ_w/σ_t) dominate the interaction mechanisms between debris flows and slit dams are when the relative post spacing is kept constant. With a lower degree of liquefaction, the grain-contact effective stress dominates. Force chains are much easier to be formed and the internal shearing of solid grains is enhanced. On the contrary, with a high degree of liquefaction, the effective stress of debris flows decreases. Thus the basal resistance becomes minor, leading to highly mobile of debris flow.

Acknowledgements

The authors acknowledge the financial support from the National Natural Science Foundation of China (grant No. 11672318), the Youth Innovation Promotion Association, CAS, and the Chinese Academy of Sciences (CAS) Pioneer Hundred Talents Program. The financial support from research grant T22-603/15-N provided by the Research Grants Council of the Government of Hong Kong SAR, China is also greatly appreciated.

References

Chanson, H., 2004, Sabo check dams-mountain protection systems in Japan: Internal Journal of River Basin Management, v. 2, no. 4, p. 301-307, doi: 10.1080/15715124.2004.9635240.

Chehata, D., Zenit, R., and Wassgren, C.R., 2003, Dense granular flow around an immersed cylinder: Physics of Fluids (1994-present) v. 15, no. 6, p. 1622-1631, doi: 10.1063/1.1571826.

Choi, C.E., Ng, C.W.W., Song, D., Kwan, J.H.S., Shiu, H.Y.K., Ho, K.K.S., and Koo, R.C.H., 2014, Flume investigation of landslide debris–resisting baffles: Canadian Geotechnical Journal, v. 51, no. 5, p. 540-553, doi: 10.1139/cgj-2013-0115.

Choi, C.E., Ng, C.W.W., Au-Yeung, S.C.H., and Goodwin, G., 2015, Froude characteristics of both dense granular and water flows in flume modelling: Landslides, v. 12, no. 6, p. 1197-1206.

Choi, S.K., Lee, J.M., and Kwon, T.H., 2018, Effect of slit-type barrier on characteristics of water-dominant debris flows: small-scale physical modelling: Landslides, v. 12, no. 6, p. 111-122.

Cui, P., Zeng, C., and Lei, Y., 2015, Experimental analysis on the impact force of viscous debris flow: Earth Surface Processes and Landforms, v. 40, no. 12, p. 1644-1655, doi: 10.1002/esp.3744.

Han, W., and Ou, G., 2006, Efficiency of slit dam prevention against non-viscous debris flow: Wuhan University Journal of Natural Sciences, v. 11, no. 4, p. 865-869.

Hauksson, S., Pagliardi, M., Barbolini, M., and Jóhannesson, T., 2007, Laboratory measurements of impact forces of supercritical granular flow against mast-like obstacles: Cold Regions Science and Technology, v. 49, no. 1, p. 54-63, doi: 10.1016/j.coldregions.2007.01.007.

Hübl, J., Suda, J., and Proske, D., 2009, Debris flow impact estimation, *in* Proceedings, The 11th international symposium on water management and hydraulic engineering, Ohrid, Macedonia, September 2009, Volume WMHE2009, p. 137-148 .

Hürlimann, M., McArdell, B.W., and Rickli, C., 2015, Field and laboratory analysis of the runout characteristics of hillslope debris flows in Switzerland: Geomorphology, v. 232, p. 20-32, 10.1016/j.geomorph.2014.11.030.

Iverson, R.M., 1997, The physics of debris flows: Reviews of geophysics, v. 34, no. 3, p. 244–296, doi: 10.1029/97RG00426.

Iverson, R.M., Logan, M., LaHusen, R.G., and Berti, M., 2010 The perfect debris flow? Aggregated results from 28 large-scale experiments: Journal of Geophysical Research: Earth Surface, v. 115, no. F03005, doi: 10.1029/2009JF001514.

Johnson, P.A., and McCuen, R.H., 1989, Slit dam design for debris flow mitigation: Journal of Hydraulic Engineering, v. 115, no. 9, p. 1293-1296, doi: 10.1061/(ASCE)0733-9429(1989)115:9(1293).

Lien, H.P., and Tsai, F.W., 2000, Debris flow control by using slit dams: International Journal of Sediment Research, v. 15, no. 4, p. 391-409.

Lien, H.P., 2003, Design of slit dams for controlling stony debris flows: International Journal of Sediment Research, v. 18, no. 1, p. 74-87.

Lin, Y.Y., and Jiang, Y.Z., 1988, Experimental study on the effectiveness of slit dam on debris flow: Journal of Chinese soil and water conservation, v. 19, no. 1, p. 40-57 (in Chinese).

Mizuyama, T., Suzuki, H., Oikaka, Y., and Morita, A., 1988, Experimental study on permeable sabo dam: Journal of Japan erosion control engineering society. v. 41, no. 2, p. 21-25 (in Japanese).

MLR (Ministry of Land and Resources), 2004, Design standards for debris flow hazard mitigation measures (DZ/T0239-2004), Beijing, China: Chinese Geological Survey, Ministry of Land and Resources (in Chinese).

McArdell, B.W., Bartelt, P., and Kowalski, J.,2007, Field observations of basal forces and fluid pore pressure in a debris flow: Geophysical Research Letters, v. 34, no. 7, doi: 10.1029/2006GL029183.

Ng, C.W.W., Choi, C.E., Song, D., Kwan, J.H.S., Koo, R.C.H., Shiu, H.Y.K., and Ho, K.K.S., 2015, Physical modelling of baffles influence on landslide debris mobility: Landslides, v. 12, no. 1, p. 1-18.

Pan, H., Wang, R., Huang, J.,2013, Study on the ultimate depth of scour pit downstream of debris flow sabo dam based on the energy method: Engineering Geology, v. 160 p. 103-109, doi: 10.1016/j.enggeo.2013.03.026.

Shima, J., Moriyama, H., Kokuryo, H., Ishikawa, N., and Mizuyama, T., 2016, Prevention and Mitigation of Debris Flow Hazards by Using Steel Open-Type Sabo Dams: International Journal of Erosion Control Engineering, v. 9, no. 3, p. 135-144, doi: 10.13101/ijece.9.135.